High-field cyclotron resonance in the conduction bands of GaSb and effective-mass parameters at the L points

H. Arimoto and N. Miura
Institute for Solid State Physics, University of Tokyo, Roppongi, Tokyo, Japan

R. J. Nicholas, N. J. Mason, and P. J. Walker
Clarendon Laboratory, University of Oxford, Parks Road, Oxford, United Kingdom

(Received 16 April 1998)

We have observed infrared cyclotron resonance in the conduction band at both the Γ and the L points in n-type GaSb at high magnetic fields up to 500 T. We observed cyclotron resonance signals from the Γ and the L points separately for temperatures higher than 100 K. The resonance at the L point was observed in fields higher than 60 T. From the photon-energy dependence of the effective mass for magnetic fields parallel to the $\langle 100 \rangle$ and the $\langle 111 \rangle$ directions, we obtained the longitudinal and the transverse effective masses, m_l and m_t, as $(1.4\pm 0.2)m_0$ and $(0.085\pm 0.006)m_0$ at the band edge of the L point. The magnetic-field-induced Γ-L crossover was estimated to take place at approximately 125 T for magnetic fields parallel to the $\langle 100 \rangle$ direction from the field dependence of the absorption intensity at the Γ and the L points and a calculation of the $N=0$ Landau levels at the Γ and the L points. The nonparabolicity at the L point is found to be larger than that at the Γ point. For the Γ point, we obtained a band-edge mass of $0.039m_0$ from the photon-energy dependence of the effective mass. [S0163-1829(98)10431-9]

I. INTRODUCTION

GaSb is known to have a conduction minimum at the Γ point, but the minima at the L point are very closely located just above the Γ minimum $[\Delta E(L\text{-}\Gamma)\sim 86\text{ meV at }200\text{ K}]$ (Ref. 1). The effective mass at the L point is expected to be larger than that at the Γ point. In sufficiently high magnetic fields, we can expect that the $N=0$ Landau level at the L point would become the lowest Landau level above the crossing point (Γ-L crossover) and the effective mass parameters at the L point would be revealed.

Recently, intersubband absorption at the L bands in GaSb-family quantum wells has been attracting much interest for normal incidence infrared devices, such as photodetectors,[2] electro-optical modulators,[3] and second-harmonic generators.[4] For a conduction band with a spherical constant-energy surface, the selection rules forbid intersubband absorption for normally incident light. For a conduction band with an ellipsoidal constant-energy surface, such as the L band of GaSb, intersubband absorption for normally incident light is allowed, when the growth direction is misaligned with respect to the principal directions of an ellipsoid. The exact values of the effective mass parameters are necessary to design these devices. Many experiments have been made to determine the longitudinal and the transverse masses, m_l and m_t, at the L point, such as the Hall effect,[5] piezoresistance (PR),[6] Faraday rotation (FR) (Ref. 7), and Shubnikov–de-Haas (SdH) effect.[8] However, there is a large scatter among the values. The reasons for the large scatter are (a) The former three methods are not resonant methods. (b) The signals are a mixture of two series arising from the Γ and the L points. (c) The mobility of the L point is not so high $(\sim 500\text{ cm}^2/\text{V s})$, so that the oscillations of SdH can be clearly observed only in high magnetic fields.

In this paper, we study infrared cyclotron resonance (CR) in the conduction band of GaSb both at the Γ and the L points in very high magnetic fields up to 500 T produced by the single-turn coil technique and electromagnetic flux compression. We observed CR signals from the Γ and the L points separately. The condition $\omega_c\tau>1$ necessary for the observation of the CR peak is readily satisfied even for the L-band carriers owing to the high magnetic fields. The CR signals from the Γ point are analyzed by the three-level model[9] and the effective mass at the band edge is determined. From CR measurements for the magnetic fields parallel to the $\langle 100 \rangle$ and $\langle 111 \rangle$ directions, m_l and m_t at the band edge of the L points are obtained.

II. EXPERIMENTAL PROCEDURE

CR experiments were performed in high magnetic fields up to 500 T by electromagnetic flux compression and up to

TABLE I. Wavelengths of the lasers and the detectors employed in this study.

λ (μm)	$\hbar\omega_c$ (meV)	Laser	Detector
119	10.4		
96.5	12.8	CO_2 pumped	Ge(Ga)
70.5	17.6	CH_3OH	
44.5	27.9		
28.0	44.3		
23.4	53.0	H_2O	Ge(Cu)
16.9	73.4		
9–11	113–138	CO_2	HgCdTe
5–6	207–248	CO	

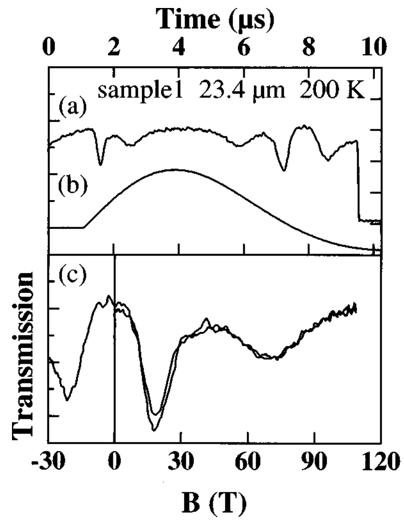

FIG. 1. Wave forms of (a) transmission and (b) magnetic field by the single-turn coil technique. (c) Transmission trace as a function of the magnetic fields.

180 T generated by the single-turn coil technique.[10] Electromagnetic flux compression generates megagauss fields by compression of the seed field by an imploding liner (copper ring) by the primary pulse current through a primary coil. This method can generate very high fields up to 550 T, but samples are destroyed at every shot. The single-turn coil technique produces megagauss fields by the direct discharge of a 100-kJ, 40-kV very fast capacitor bank into single-turn copper coils with a diameter of 8–18 mm. Maximum fields are obtained before the destruction of the coil. The coil and its clamping system are enclosed in a large steel box to protect the optical apparatus from the scattering pieces of the destroyed coil and to shield the detector from the noise generated by the explosion of the coil. The advantage of this method is that samples and cryostats are not damaged by the shot, despite the violent coil destruction. The absolute field strength was determined to an accuracy of better than 2% by measuring the induced voltage in a pick-up coil wound around the sample. The pick-up coil was calibrated by comparison with a standard coil whose sensitivity is accurately known.

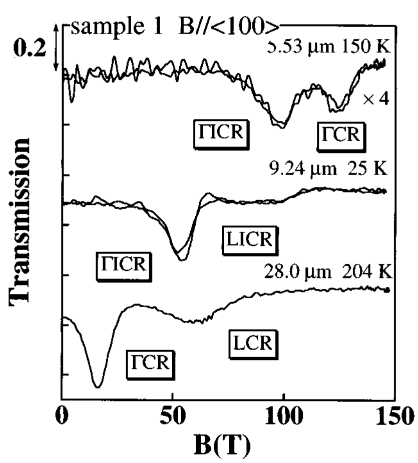

FIG. 2. CR traces for sample 1 at three different wavelengths for the field parallel to the ⟨100⟩ direction. ΓCR, ΓICR, *L*CR, and *L*ICR denote the CR and the impurity CR at the Γ point, and those at the *L* points, respectively.

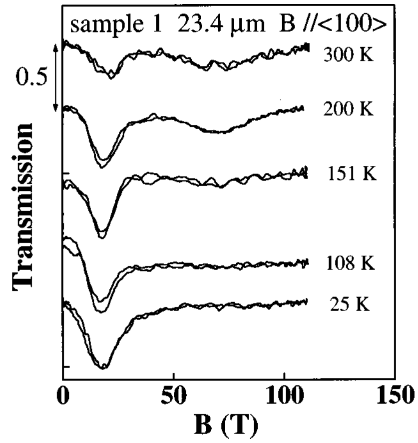

FIG. 3. CR traces for sample 1 at a wavelength of 23.4 μm from 25 to 300 K.

As far-infrared and infrared radiation sources, we employed various molecular gas lasers. They are listed in Table I together with the wavelengths employed in this study and detectors suitable for each wavelength.

GaSb thin single crystals were grown on (100) GaAs substrates by the metal-organic vapor-phase epitaxy technique at the Clarendon Laboratory in Oxford. Selenium doping was used to provide conduction electrons. Electron concentration and thickness of the samples are 30×10^{16} cm^{-3}, 2.1 μm for sample 1 and 5.5×10^{16} cm^{-3}, 6 μm for sample 2. The sample temperature was controlled from 10 K to room temperature by flowing liquid helium in the cryostat. The temperature was measured by a thermocouple placed near the sample.

Figure 1 shows the wave forms of magnetic field and transmission by the single-turn coil technique. Despite the violent coil destruction, its effect is not seen in both traces. Resonance peaks are observed twice in the transmission signal, one corresponding to the up sweep and the other corresponding to the down sweep. At low fields, the third resonance is observed in the reverse fields. It should be noted that a good coincidence for the sweeps ensures the accuracy of the measurement.

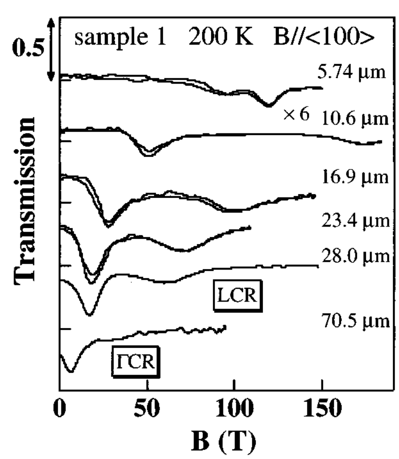

FIG. 4. CR traces for various wavelengths at 200 K.

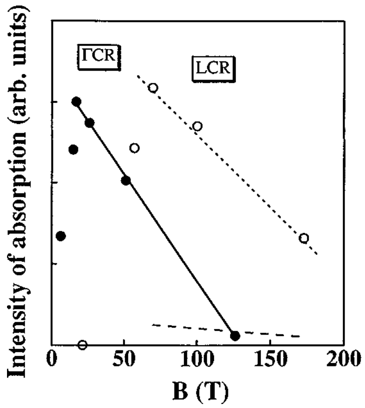

FIG. 5. Field dependence of the absorption intensity from the Γ and the L points. The solid and dotted lines are guide lines for the Γ and the L points, respectively. The dashed line is one-thirteenth of the dotted line. The crossing point of the dotted and the dashed lines is the field where the field-induced Γ-L crossover is expected to take place.

III. RESULTS AND DISCUSSION

Figure 2 shows typical CR traces at various wavelengths for the field parallel to the ⟨100⟩ direction. At 28 μm, a clear absorption peak from the Γ point was observed at 16.9 T, which gives an effective mass of $0.044m_0$. A broader but well-defined peak from the L points was observed at 59.1 T, from which we obtain the effective mass of the L point as $0.156m_0$. At 5.53 μm, two peaks from the Γ point, the intensity of which is much smaller than that at 28 μm, were observed. The absorption intensity at the lower fields decreased with the increase of temperature, so this peak is attributed to the impurity cyclotron resonance (ICR), which is the transition between the (000) and the (010) states in the $(NM\lambda)$ notation or the $1s\rightarrow 2p+$ transition in the terminology of hydrogen atom model. The higher field peak at 129 T is the spin-plus CR, which gives an effective mass of $0.067m_0$. This value is about 50% larger than that at 28 μm, indicating a large nonparabolicity at the Γ point. GaSb is usually classified as a medium gap semiconductor with $E_g \sim 0.8$ eV. However, GaSb can behave as a narrow-gap semiconductor and exhibit a large nonparabolicity and a large spin splitting in high-field CR at 5.53 μm, because the photon energy is about 224 meV and is almost one-third of the band-gap energy. The spin-minus CR was not observed, because the splitting of spin-plus and spin-minus $N=0$ Landau levels is very large due to the large g_0^* value $(=-7.68)$ (Ref. 11) and the intense magnetic fields, so that the carriers depopulate in the spin-minus state. At 9.24 μm, the ICR at the Γ (ΓICR) and the L points (LICR) were observed at low temperature.

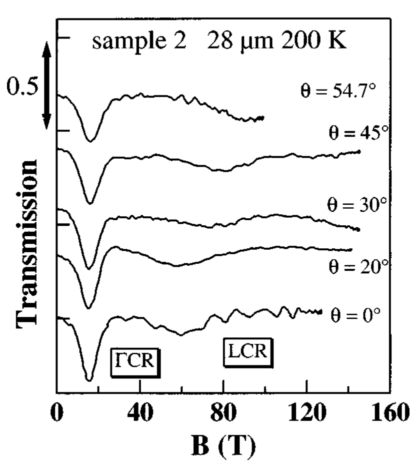

FIG. 6. CR traces of sample 2 for various tilt angles θ from the ⟨100⟩ direction in the (110) plane.

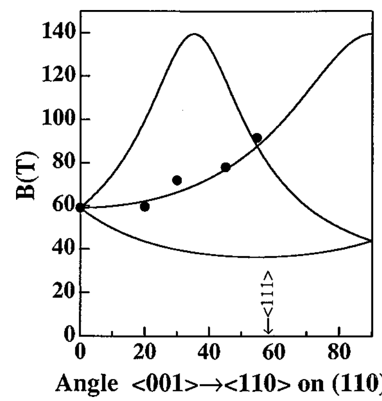

FIG. 7. Angular dependence of the effective masses at the L points. The solid lines are the theoretically expected curves with $m_l=1.4m_0$ and $m_t=0.095m_0$.

Temperature dependence of the CR traces is shown in Fig. 3. The peak from the L points weakens at temperatures below 100 K due to the freeze-out effect to the deep donor level at the Γ and the L points.

Figure 4 shows the CR traces for various wavelengths at 200 K. A large photon energy dependence of the absorption intensity was found for both the Γ and L points. Figure 5 shows the field dependence of the absorption intensity from both the Γ and L points. The absorption intensity from the Γ point became smaller with the increase of the resonant field, whereas the absorption intensity from the L points increased in fields lower than 70 T. The decrease of the absorption intensity from the L points in fields higher than 70 T results from magnetic freeze-out to the impurity level associated

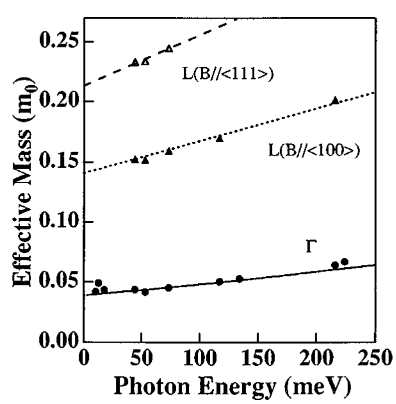

FIG. 8. Field dependence of effective masses at the L point for $B\|\langle 100\rangle$ and $B\|\langle 111\rangle$, together with the effective mass at the Γ point. The dashed and dotted lines are the calculated values from the effective two level model for $B\|\langle 100\rangle$ and $B\|\langle 111\rangle$, respectively. The solid line represents the calculated values from the three level model for the ΓCR.

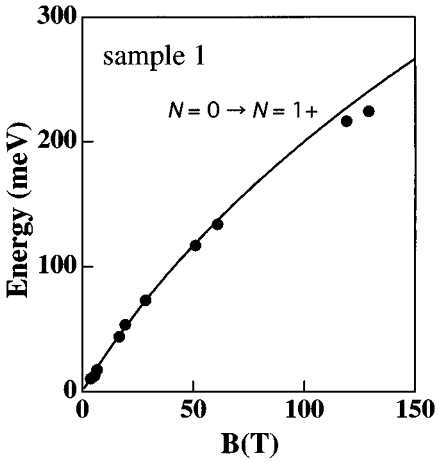

FIG. 9. ΓCR peak position of sample 1. Solid line is the calculated transition energy for spin-plus electron by the 3LM.

with the Γ and the L point. The crossover of the absorption intensity indicates the fast electron transfer from the Γ to the L points as a result of the approach of the L extrema to the Γ extremum. A coincidence of the spectra for the up-sweep and the down-sweep fields also indicates that the carrier transfer is faster than the sweep time of the megagauss field, which is of the order of several μs. The carrier transfer time from the Γ to the L points has already been estimated to be less than 50 fs by optical transmission-correlation spectroscopy.[12] Considering the four equivalent valleys of the L point and the effective-mass difference, the density of states at the L extrema is 13 times larger than that at the Γ extremum. Using this, we can estimate that the field for the Γ-L crossover is about 125 T. For a more accurate evaluation, we should take into account the transition probability.

In order to separate the longitudinal and the transverse masses, m_l and m_t, at the L point, we tilted the magnetic-field direction in the (110) plane. Figure 6 shows the CR traces for various tilt angles θ for 28 μm. We observed a clear shift of the peak. The observed angular dependence of the effective masses is shown in Fig. 7. The data are fitted using effective-mass parameters of $m_l^* = 1.4m_0$ and $m_t^* = 0.095m_0$. Relatively good agreement is found for the m_2 branch, which ensures that the absorption originates from the L points. The reasons why the other two branches were not observed are (a) a sufficiently large number of carriers do not exist for observing the CR signals at the m_1 branch because the Γ-L crossover does not occur at low fields; (b) the m_2 branch has two equivalent L valleys, whereas the m_1 and the m_3 branches come from a single valley. The theoretical curves are insensitive to the value of m_l. As shown below, the nonparabolicity at the L points is very large, so it is not appropriate to fit the data with fixed parameters. For these reasons, we use another method to determine m_l and m_t. We measured CR for B parallel to the ⟨100⟩ and ⟨111⟩ directions. The field dependence of the effective masses at the L point for $B \| \langle 100 \rangle$ and $B \| \langle 111 \rangle$ are shown in Fig. 8 together with the effective mass at the Γ point. By fitting the data with the transition energy obtained from an effective two-level model, we estimate the effective masses at the band edge as $0.14m_0$ for $B \| \langle 100 \rangle$ and $0.21m_0$ for $B \| \langle 111 \rangle$. We compared the experimental dispersion curve with the two level model, with the energy gap as an adjustable parameter. The best fit E_g^* values for $B \| \langle 100 \rangle$ and ⟨111⟩ are 1.13 and 1.05 eV. These values are nearly half of the actual energy gap (2.1 eV) at the L point. From these effective masses, we obtain $m_l = (1.4 \pm 0.2)m_0$ and $m_t = (0.085 \pm 0.006)m_0$ at the band

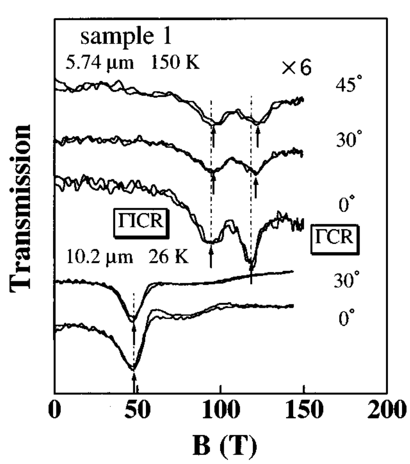

FIG. 10. CR traces of sample 1 for different tilt angles at 5.74 and 10.2 μm. The magnetic field is tilted from the ⟨100⟩ direction in the (110) plane.

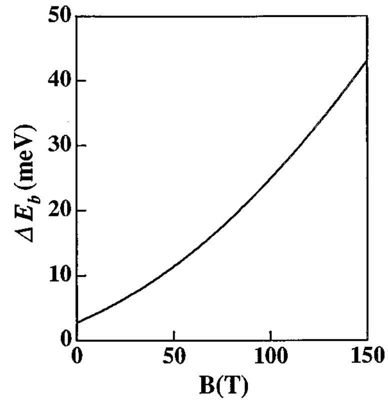

FIG. 11. ΔE_b as a function of magnetic field. ΔE_b is a difference in energy between the ΓCR and the ΓICR which are fitted by suitable polynomials.

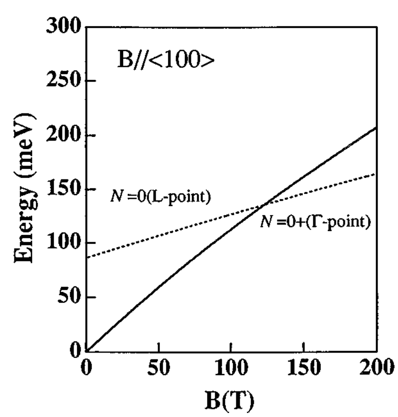

FIG. 12. The calculated values of the $N=0$ Landau level at the Γ (solid line) and the L points (dotted line) for $B \| \langle 100 \rangle$. The values for the Γ point are obtained from the 3LM, whereas the values for the L points are derived from the effective two-level model.

TABLE II. Effective masses as the Γ point.

λ (μm)	$\hbar\omega_c$ (meV)	m^*/m_0	Methods	Reference
Band edge		0.039±0.001	CR	Present work
28.0	44.3	0.044±0.001	CR	Present work
10.6	117	0.050±0.001	CR	Present work
5.53	224	0.067±0.001	CR	Present work
88	14.1	0.0412	CR	Ref. 15
		0.041	Shubnikov–de Haas	Ref. 11

edge. It should be noted that the nonparabolicity at the L point is much larger than at the Γ point, contrary to the expectation from simple $k\cdot p$ theory. A large nonparabolicity at the L point has been also reported for Ge (Ref. 13) and the reason is not clear at this moment.

The photon energy dependence of ΓCR is plotted as a function of the magnetic fields in Fig. 9. By fitting the CR data with the transition energy obtained from the three-level model (3LM), we estimate the effective mass for the band edge of the Γ point as $0.039m_0$. This value is in good agreement with the previously reported value by CR.[15] Values employed in the calculation are $E_g=0.762$ eV,[1] $\Delta=0.78$ eV (spin-orbit splitting),[14] $g_0^*=-7.68$.[11] In fields lower than 60 T, the calculated values are in good agreement with the experiment, but a disagreement becomes prominent at approximately 125 T. We deduce two reasons for the disagreement. One is that in high magnetic fields, the 3LM analysis is not sufficient and we have to take into account the higher conduction bands, Γ_{8c} and Γ_{7c}. In the case of GaAs, which has relatively wide gap (1.5 eV), the CR positions at high magnetic fields were compared with the five-level model and a reasonable agreement was found.[16,17] Another reason is that the wave function at the Γ point is influenced by the wave function at the L points and the effective mass becomes resonantly larger at the Γ-L crossover field of 125 T. The influence of the L points on the Γ point was also found in the angular dependence of ΓCR at around 125 T. Figure 10 shows the CR traces for various tilt angles θ for 5.74 μm and 10.2 μm. The ΓICR peaks at 50 T for 10.2 μm and at 90 T for 5.74 μm were almost independent of the tilt angle, indicating a spherical effective mass at the Γ point. For 5.74 μm, the CR peak at approximately 120 T for $\theta=45°$ was at about 3% higher fields than for $\theta=0°$. It is possible that this anisotropy of the effective mass at the Γ point might be caused by the interaction of the wave function at the Γ point with the anisotropic wave function at the L point.

Figure 11 shows the difference in energy between ΓCR and ΓICR, ΔE_b, as a function of magnetic field. We obtained ΔE_b by fitting the experimental data of the ΓCR and the ΓICR to suitable polynomials, respectively. ΔE_b is equal to the difference in the binding energy between the (000) and the (010) states, associated with the $N=0$ and $N=1$ Landau levels, respectively. The steep increase of ΔE_b cannot be explained by the hydrogenic atom model in the presence of B even including the effect of the band nonparabolicity, which explains well ICR in InSb (Ref. 18) and GaAs.[19] This indicates that we have to include the effect of the chemical shift. In the simplest model, the chemical shift is proportional to the possibility of finding an electron around the impurity atom and is important only for the binding energy of the (000) state. For the (010) state that consists of much more extended p-like wave functions, the chemical shift is small. So we can attribute the field dependence of ΔE_b to the field dependence of the chemical shift of the (000) state. If we take into account only the effect of the wave function shrinkage around the impurity atom in the plane perpendicular to B, the increase of the chemical shift of the (000) state should be roughly proportional to B. We deduce that one of the reasons for the stronger dependence of

TABLE III. Effective masses at the L point.

	λ (μm)	$\hbar\omega_c$ (meV)	m^*/m_0	Methods	Reference
$m^*\langle 100\rangle$	Band edge		0.14±0.01	CR	Present work
	28.0	44.3	0.150±0.002	CR	Present work
	10.6	117	0.170±0.002	CR	Present work
$m^*\langle 111\rangle$	Band edge		0.21±0.01	CR	Present work
	16.9	73.4	0.243±0.002	CR	Present work
m_t	Band edge		0.085±0.006	CR	Present work
m_l	Band edge		1.4±0.2	CR	Present work
m_t			0.14	FR	Ref. 7
m_l			1.2	FR	Ref. 7
m_t			0.12	PR	Ref. 6
m_l			1.3	PR	Ref. 6
m_t			0.285	SdH	Ref. 8
m_l			2.8	SdH	Ref. 8

ΔE_b on the magnetic fields is the shrinkage of the wave function along the direction of the magnetic field. It is very difficult to find a numerical agreement between the experimentally obtained ΔE_b and the calculated values of the chemical shift, because (a) there is no calculation of the chemical shift in magnetic fields for the (000) state that has a large chemical shift comparable to the effective Rydberg energy such as Se in GaSb and (b) there is no report of the shallow donor state connected with the Γ point in GaSb. However, the steep increase of ΔE_b indicates a large chemical shift of the (000) state of Se in GaSb, which we deduce should be larger than the effective Rydberg energy of GaSb (2.2 meV) and be the dominant factor of ΔE_b. The effective masses obtained in the present study at various wavelengths are listed in Table II and Table III together with the values reported in previous papers for comparison.

The calculated values of the $N=0$ Landau level at the Γ and the L points for $B\|\langle 100\rangle$ are shown in Fig. 12. The values for the Γ point are obtained from the 3LM, whereas the values for the L point are derived from the effective two-level model. Adopting the value of $\Delta E(L\text{-}\Gamma)$ as 86 meV at 200 K,[20] the Γ-L crossover takes place at 123 T. This value is in good agreement with the field obtained from the field dependence of the absorption intensity.

IV. CONCLUSION

We have observed infrared (5–119 μm) CR in the conduction band in *n*-type GaSb(Se) at high magnetic fields up to 500 T. We observed CR from the Γ and L points separately. The resonant field dependence of the absorption intensity from the Γ and L points revealed that the field-induced Γ-L crossover takes place at around 125 T for $B\|\langle 100\rangle$. We observed CR from the L points with B parallel to the $\langle 100\rangle$ and $\langle 111\rangle$ directions and obtained $m_l=(1.4\pm 0.2)m_0$ and $m_t=(0.085\pm 0.006)m_0$ at the band edge. A large nonparabolicity was found in the L points. We compared the CR data for the Γ point with the values calculated from the 3LM and estimated the band-edge mass to be $(0.039\pm 0.001)m_0$. In fields lower than 60 T, we obtained a very good agreement between experiment and theory. However, at approximately 125 T, a small disagreement was found. We deduce that the disagreement comes from the influence of the higher conduction bands (Γ_{8c} and Γ_{7c}) and the L points that are expected to be close to the Γ point at 125 T. The influence of the L points was also seen in the angular dependence of the CR position from the Γ point. ΔE_b was found to increase steeply, indicating a large chemical shift of the (000) state of Se in GaSb. Calculation of the $N=0$ Landau level at the Γ and L point also led to a value of 123 T for the Γ-L crossover, assuming ΔE $(L\text{-}\Gamma)=86$ meV.

[1] H. J. Lee and J. C. Woolley, Can. J. Phys. **59**, 1844 (1981).
[2] Y. Zhang, N. Baruch, and W. I. Wang, Appl. Phys. Lett. **63**, 1068 (1993).
[3] J. R. Meyer, C. A. Hoffman, F. J. Bartoli, and L. R. Ram-Mohan, Appl. Phys. Lett. **67**, 2756 (1995).
[4] H. Xie, W. I. Wang, J. R. Meyer, and L. R. Ram-Mohan, Appl. Phys. Lett. **65**, 2048 (1994).
[5] J. Basinski, C. C. Y. Kwan, and J. C. Woolley, Can. J. Phys. **50**, 1068 (1972).
[6] M. Averous, G. Bougnot, J. Calas, and J. Chevrier, Phys. Status Solidi **37**, 307 (1970).
[7] H. Piller, in *Proceedings of the 7th International Conference on the Physics of Semiconductors, Paris 1964* (Dunod, Paris, 1964), p. 297.
[8] P. Perrier, J. C. Portal, J. Galibert, and S. Askenazy, J. Phys. Soc. Jpn. **49**, Suppl. A 113 (1980).
[9] B. Lax, J. G. Mavroides, H. J. Zeiger, and R. J. Keye, Phys. Rev. **122**, 31 (1961).
[10] N. Miura, Physica B **201**, 40 (1994).
[11] H. Hazama, Y. Itoh, and C. Hamaguchi, J. Phys. Soc. Jpn. **54**, 269 (1985).
[12] W. S. Pelouch and L. A. Schlie, Appl. Phys. Lett. **66**, 82 (1995).
[13] R. L. Aggarwal, M. D. Zuteck, and B. Lax, Phys. Rev. **180**, 800 (1969).
[14] M. Cardona, K. L. Shaklee, and F. H. Pallak, Phys. Rev. **154**, 696 (1967).
[15] D. A. Hill and C. F. Schwerdtfeger, J. Phys. Chem. Solids **35**, 1533 (1974).
[16] S. P. Najda, S. Takeyama, N. Miura, P. Pfeffer, and W. Zawadzki, Phys. Rev. B **40**, 6189 (1989).
[17] N. Miura, H. Nojiri, P. Pfeffer, and W. Zawadzki, Phys. Rev. B **55**, 13 598 (1997).
[18] R. Kaplan, R. A. Cooke, and R. A. Stradling, Solid State Commun. **26**, 741 (1978).
[19] P. Pfeffer, W. Zawadzki, S. P. Najda, H. Yokoi, S. Takeyama, and N. Miura, Physica B **201**, 288 (1994).
[20] M. C. Wu and C. C. Chen, J. Appl. Phys. **72**, 4275 (1992).